

# CHAPTER I

## INTRODUCTION

### 1.1 Functional Coordination Polymers with Stable pores<sup>1,2</sup>

In the last decade coordination compounds with infinite one-, two-, and three-dimensional (1-, 2-, and 3D) network structures have been intensively studied. In particular, compounds with backbones constructed by metal ions as “**nodes**” and ligands as “**linkers**” form a family of polymers, which are called “coordination polymers”.<sup>3</sup> The key to the rational synthesis to realize a certain desired framework is the judicious choice of metal ion(s), ligand(s), and framework motifs. In addition, that the architecture of coordination polymers can be reasonably well predicted rests upon the simple premise that the coordination geometry of metal ions can be propagated with rigid bridging ligands.<sup>4</sup> It is therefore unsurprising that a wide range of 1D, 2D, and 3D infinite frameworks has already been generated with simple, linear linkers such as **4,4'-bpy** (4,4'-bipyridine). On the basis of this achievement as to what researchers call “first generation compounds”, in principle, a wide variety of chemical and/or physical properties, such as catalytic, magnetic, electrical, and optical properties, might be rationally put in such frameworks.

In particular, porous coordination polymers have attracted the attention of chemists, due to scientific interest in the creation of nanometer-sized spaces and the finding of novel phenomena as well as commercial interest in their application in separations, storage, and heterogeneous catalysis.<sup>1</sup> In 1998, porous coordination compounds were first classified in the three categories, 1<sup>st</sup>, 2<sup>nd</sup> and 3<sup>rd</sup> generation.<sup>5</sup> The 1<sup>st</sup> generation compounds have microporous frameworks, which are sustained only with guest molecules and show irreversible framework collapse on removal of guest molecules. The 2<sup>nd</sup> generation compounds have stable and robust porous frameworks, which show permanent porosity without any guest molecules in the pores. The 3<sup>rd</sup> generation compounds have flexible and dynamic frameworks, which may respond to external stimuli, such as light, electric field, guest molecules, and change their channels or pores reversibly. Many inorganic porous materials constructed by covalent bonds are classified as 2<sup>nd</sup> generation compounds. On the other hand, porous coordination polymers could afford not only robust “2<sup>nd</sup>

generation compounds”, but also flexible and dynamic “3<sup>rd</sup> generation ones”. Figure 1.1 shows the advent of chemical/physical properties in chronological order. These results stimulated to search for unique functions for guest adsorption, which, in certain cases, are beyond the scope of the zeolites and activated carbons. This new feature is associated with their complete regularity, high porosity, and highly designable frameworks. One can take advantage of the fact that in the synthesis the reactions occur under mild conditions and the choice of a certain combination of discrete molecular units leads to the desired extended network.<sup>6–8</sup> Recent activity in crystal engineering has afforded several examples of coordination polymers which have rigid open frameworks, and therefore have the potential to be functionally related to zeolites. The  $[\text{Cu}(\text{SiF}_6)(4,4'\text{-bpy})_2]_n$  was reported as a prototype in the context of coordination polymers since it can be regarded as having been generated from square-grid coordination polymers that are cross-linked by  $\mu\text{-SiF}_6$  anions.<sup>9</sup> Also,  $[\text{Zn}_4\text{O}(\text{BDC})_3]_n$  BDC = benzenedicarboxylic acid was synthesized on the basis of the ideas from metal carboxylate supported polynuclear core chemistry, where an organic dicarboxylate linker is used in a reaction that gives supertetrahedron metal cores capped with monocarboxylates.<sup>10</sup> This porous coordination polymer was realized by utilizing the geometrical shapes of the metal cores relative to secondary building units (SBUs).<sup>10</sup>

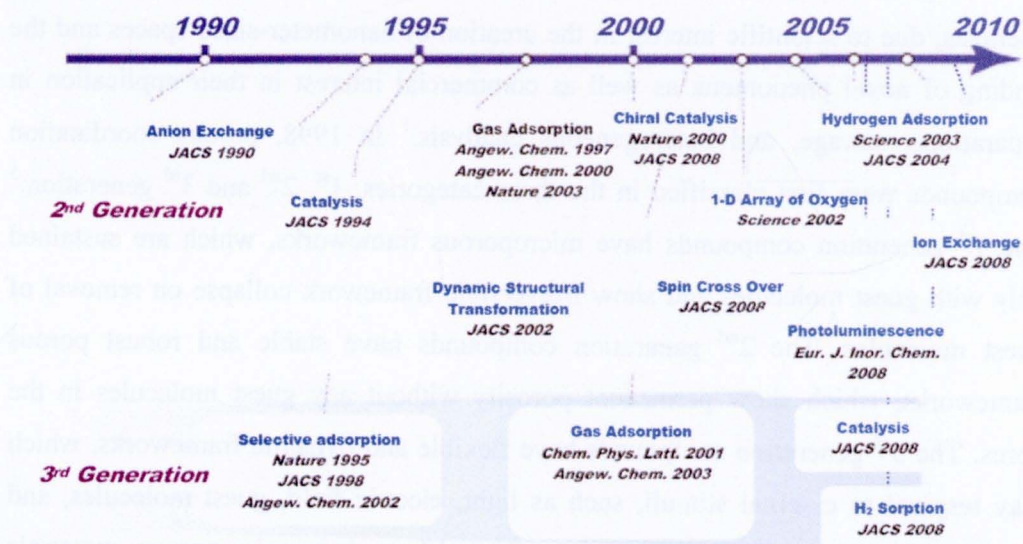


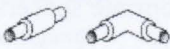
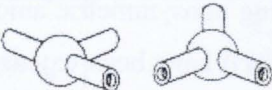
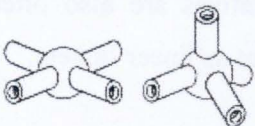
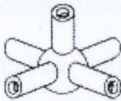
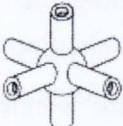
**Figure 1.1** Historical view of functions of coordination polymers reported from 1990 to the present day drawn after reference 1.

Both these compounds contain added linkers of rigid and divergent characters, which allow articulation into a 3D framework, resulting in a structure with higher apparent surface area and pore volume. Over the past decade a considerable number of studies have been made on the synthesis of thermally stable and robust 3D frameworks without guest molecules, in order to determine porous functionalities.<sup>4,8-10</sup> This is the second achievement in coordination polymers, and therefore researchers call them “second generation compounds”.<sup>5</sup>

## 1.2 Principles in Synthesis<sup>1</sup>

### 1.2.1 Connectors and Linkers

Coordination polymers contain two central components, connectors and linkers. These are made from the starting reagents with which the principal framework of the coordination polymer is constructed. In addition, there may be other auxiliary components, such as blocking ligands, counteranions, and nonbonding guests or template molecules (Figure 1.2). The important characteristics of connectors and linkers are the number and orientation of their binding sites (coordination numbers and coordination geometries).

Number of functional sites	Connectors	Linkers
2		
3		
4		
5		
6		

**Figure 1.2** Components of coordination polymers.

Transition-metal ions are often utilized as versatile connectors in the construction of coordination polymers. Depending on the metal and its oxidation state, coordination numbers can range from 2 to 10, giving rise to various geometries, which can be linear, T- or Y-shaped, tetrahedral, square-planar, square-pyramidal, trigonal-bipyramidal, octahedral, trigonal-prismatic, and the corresponding distorted forms (Figure 1.2). The large coordination numbers from 7 to 10 and the polyhedral coordination geometry of the lanthanide ions are useful for the generation of new and unusual network topologies. In addition, coordinatively unsaturated lanthanide ion centers can be generated by the removal of coordinated solvent molecules. The vacant sites could be utilized in chemical adsorption, heterogeneous catalysis, and sensors.<sup>11</sup> Instead of a naked metal ion, the metal-complex connectors have the advantage of offering control of the bond angles and restricting the number of coordination sites; sites that are not required can be blocked by chelating or macrocyclic ligands that are directly bound to a metal connector, and thus leave specific sites free for linkers.

Linkers afford a wide variety of linking sites with tuned binding strength and directionality (Figure 1.3). Halides (F, Cl, Br, and I) are the smallest and simplest of all linkers. The most frequently used neutral organic ligands are pyrazine (pyz) and 4,4'-bpy.<sup>12</sup> Recent efforts have been devoted to utilization of long bridging ligands with appropriate spacers.<sup>13</sup>

Di-,<sup>14</sup> tri-,<sup>15</sup> tetra-,<sup>16</sup> and hexacarboxylate<sup>17</sup> molecules are typical anionic linkers. Coordination polymers having nonsymmetric anionic ligands (generally described as pyridine-X-COO<sup>-</sup> (X = spacer)) have been extensively studied.<sup>18</sup> 1,4-Dihydroxy-2,5-benzoquinone and its derivatives are also often used and give rise a variety of frameworks, in which they act as linear linkers.

### 1.2.2 Design of Motifs

Excellent reviews about the structural topologies of the frameworks of coordination polymers and/or inorganic materials have been published,<sup>1,2</sup> and, therefore, topological features are only described briefly in this section.

Various combinations of the connector(s) and linker(s) mentioned in the previous section afford various specific structural motifs. Figure 1.4 shows representative motifs of frameworks constructed from various types of connectors and

a linear linker. A linear chain is a simple 1D motif. The Ag(I) ion tends to form a linear chain with several linear linkers as a result of its preference for a coordination number of two.<sup>7</sup>

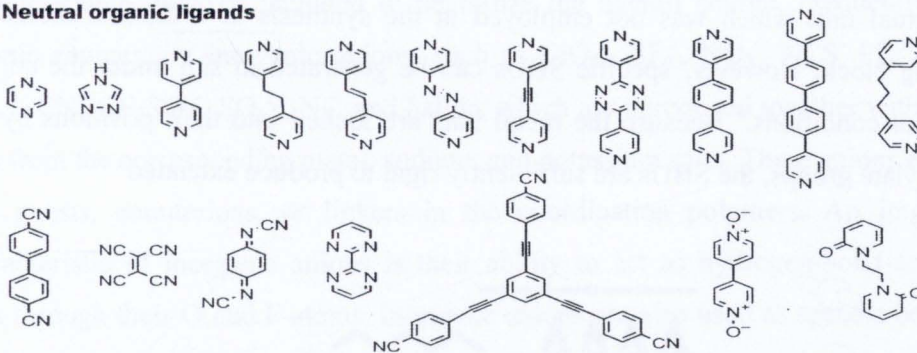
### (a) Inorganic ligands

Halides (F, Cl, Br, and I)

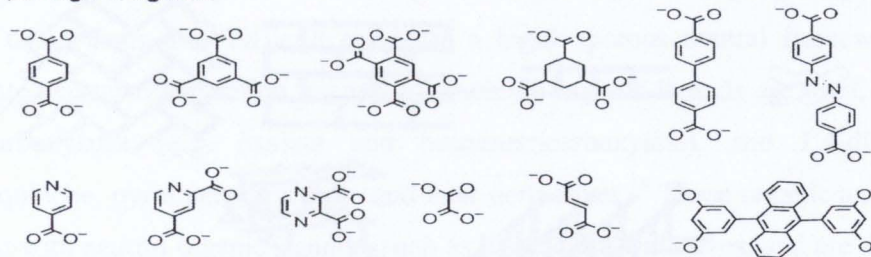


Cyanometallate ( $[\text{M}(\text{CN})_x]^{n-}$ )

### (b) Neutral organic ligands



### (c) Anion organic ligands



### (d) Cation organic ligands

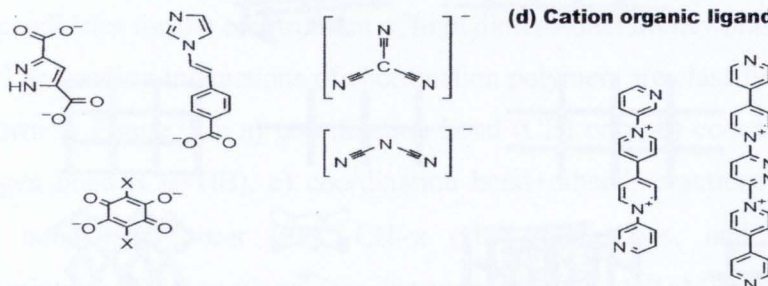


**Figure 1.3** Examples of linkers used in coordination polymers.

The synthesis of homochiral, porous materials is a particularly interesting objective, because such chiral porous coordination polymers could be of use for applications in heterogeneous asymmetric catalysis and enantioselective separations.<sup>19</sup> Strategies for forming homochiral frameworks exploit enantiopure organic ligands, or the use of helical chains or helical frameworks. The inherent chirality of this

architecture comes from spatial disposition rather than the presence of chiral centers. Polynuclear clusters constructed from two or more metal ions and multidentate carboxylate linkers, such as 1,4-bdc and 1,3,5-btc, (so-called “secondary building units” (SBUs)), can have special coordination numbers and geometries. When such polytopic units are copolymerized with metal ions, it is common to find linked cluster entities in the assembled solid. Each cluster is considered to be an SBU, in that it is a conceptual unit which was not employed in the synthesis as a distinct molecular building block. However, specific SBUs can be generated in situ under the correct chemical conditions.<sup>8</sup> Because the metal ions are locked into their positions by the carboxylate groups, the SBUs are sufficiently rigid to produce extended

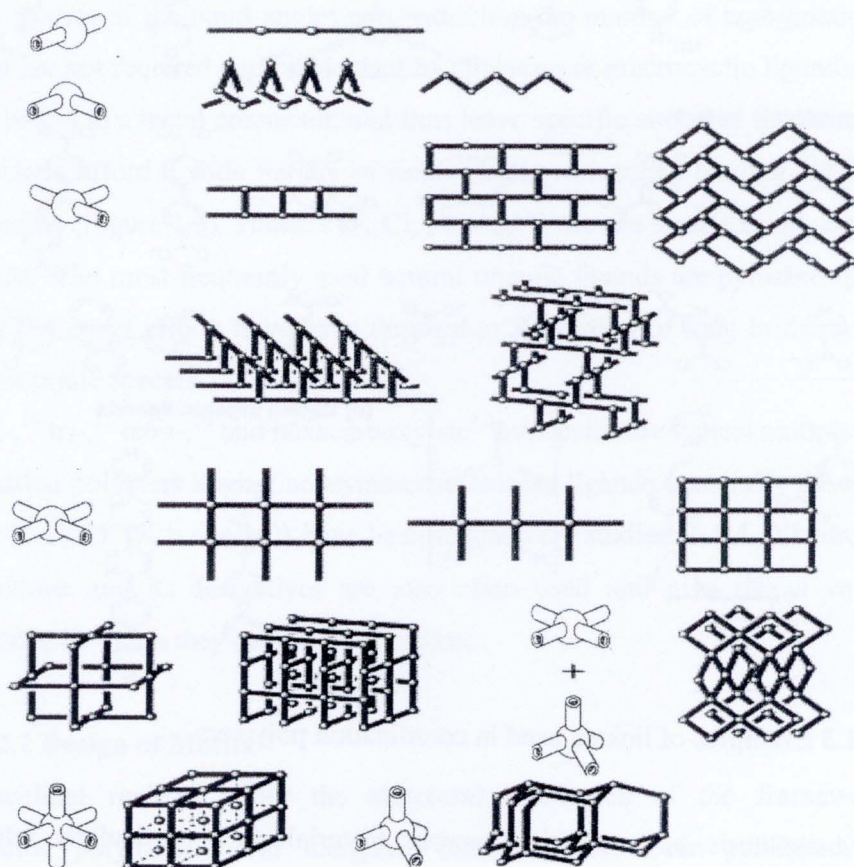


**Figure 1.4** Examples of structural frameworks that can be constructed by using different connectors and linear linkers.

frameworks of high structural stability. Such frameworks are also neutral, obviating the need for counterions in their cavities. In clusters with terminal ligands, the reactivity of the metal site can be studied through the removal of these ligands, which generates a free coordination site.

Charge is an important factor in the rational construction of functional coordination polymers. Since most of transition-metal connectors are cationic, an anionic source must be included to neutralize the overall charge. Frequently used anionic sources are inorganic anions, such as  $\text{ClO}_4^-$ ,  $\text{BF}_4^-$ ,  $\text{NO}_3^-$ ,  $\text{NCS}^-$ ,  $\text{PF}_6^-$ ,  $\text{NO}_2^-$ ,  $\text{SiF}_6^{2-}$ ,  $\text{CN}^-$ ,  $\text{CF}_3\text{SO}_3^-$ ,  $\text{SO}_4^{2-}$ ,  $\text{N}_3^-$ , and halide, which are introduced together with metal ions from the corresponding metal, sodium, and potassium salts. These anions exist as free guests, counterions, or linkers in the coordination polymers. An important characteristic of inorganic anions is their ability to act as hydrogen-bond-acceptor sites through their O and F atoms. Inorganic anions are also used as spacers between magnetic chains and layers.<sup>20</sup> However, the disadvantage of inorganic anions is that when using them it is difficult to create a highly porous neutral framework. To generate neutral coordination frameworks anionic organic ligands are used, such as polycarboxylates (e.g. oxalate and benzenetricarboxylate), and 1,4-dihydroxy benzoquinone, pyridinecarboxylate, and their derivatives.<sup>18</sup> These organic anions can coexist with neutral organic ligands, such as bipyridine derivatives, and are therefore good candidates for the construction of high dimensional frameworks.

The bonding interactions of coordination polymers are classified into four types as shown in Figure 1.5: a) coordination bond (CB) only, b) coordination bond and hydrogen bond (CB+HB), c) coordination bond+other interactions, such as metal-metal bond (MB),  $\pi$ - $\pi$  (PP), CH- $\pi$  (HP) interactions, and d) coordination bond+mixture of interactions (for instance, HB+PP, HB+MB, or MB+PP). The stability of 3D motifs increases with increasing coordination bond contribution. 1D and 2D motifs often aggregate through additional weak bonds (HB, PP, HP) to give 3D frameworks. In some cases, 1D and 2D motifs are linked by guest molecules through weak interactions. Of course, even 3D motifs interact with each other by such weak interactions (for example, when interpenetration of lattices occurs).

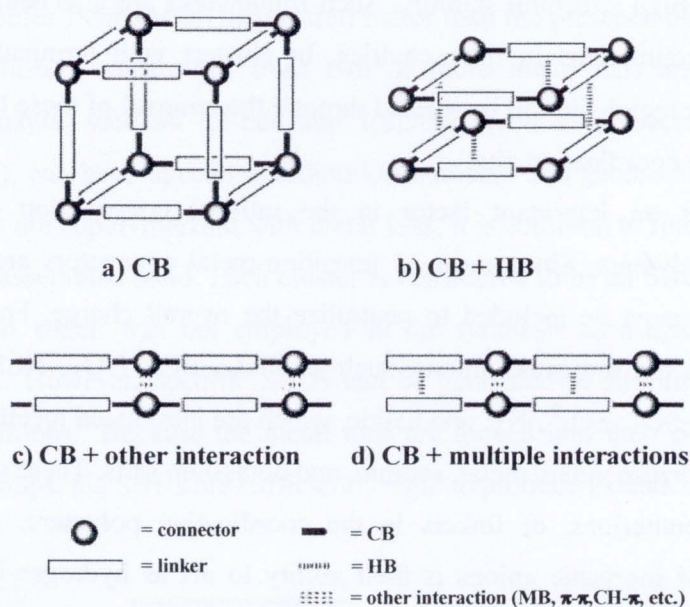


**Figure 1.5** Combinations of interactions participating in the construction of a coordination polymer.

Coordination polymers with two kinds of connectors (heterometallic polymers) are of great interest owing to their possible applications for the functionalization of micropores and/or microchannels and the construction of molecular-based magnets. Therefore, a new type of donor building block has been developed, which is a hybrid inorganic–organic bridging ligand, the so-called metalloligand.<sup>21</sup> A metalloligand has several advantages:

1) simple to prepare multifunctional ligands. Multifunctional organic bridging ligands require many intricate synthetic steps while multifunctional metalloligands can be obtained from combination of simple connectors and linkers,

2) modification of coordination ability is possible. Owing to the Lewis acidity and electrostatic effect of metal ions, the coordination properties of the functional groups in the metalloligand can be modified,

3) amphoteric properties. In addition to Lewis basic coordination sites, metalloligands also provide a Lewis acidic site at the metal ion,

4) two functions for the metal ions. Two roles of metal ions can be utilized; one is to link connectors to afford the backbone of a framework. The other is to make a branch in the backbone. This advantage also contributes to the chemical or physical

properties of the coordination polymer. Homometallic coordination polymers and also heterometallic ones can be systematically synthesized.

The immobilization of coordinatively unsaturated metal centers (UMCs) into porous frameworks is a very attractive idea, because a regular arrangement of metal centers in a certain space induces regioselectivity or shape- or size selectivity towards guest molecules. Moreover, the combination of a catalytic center with porous properties and effective isolation from species toxic to the catalyst leads to efficient tailor-made reaction systems, which approach the peptide architecture of enzymes in biological systems.<sup>22</sup> The immobilization of UMCs in porous hosts has been tried by using zeolites, polymeric matrices, and clays by means of ion exchange or impregnation. However, by these methods it was not possible to generate sufficiently isolated and uniformly distributed UMCs and the environment around the UMC is not clearly defined. If the UMC can be directly incorporated into the channel walls of microporous coordination polymers, completely isolated and uniformly distributed catalytic centers would be realized. For this purpose, a new synthetic scenario has been developed, that is, “two-step self-assembly”. First, a metalloligand is synthesized, which acts not only as a framework linker, but also as a UMC ( $M^1$ ). Second, the metalloligand is added to another metal ion ( $M^2$ ), which acts as a node in the framework. Consequently, two kinds of metal centers coexist in a framework (Figure 1.6), and the metal ion in the channel wall presents a large surface to guest molecules.

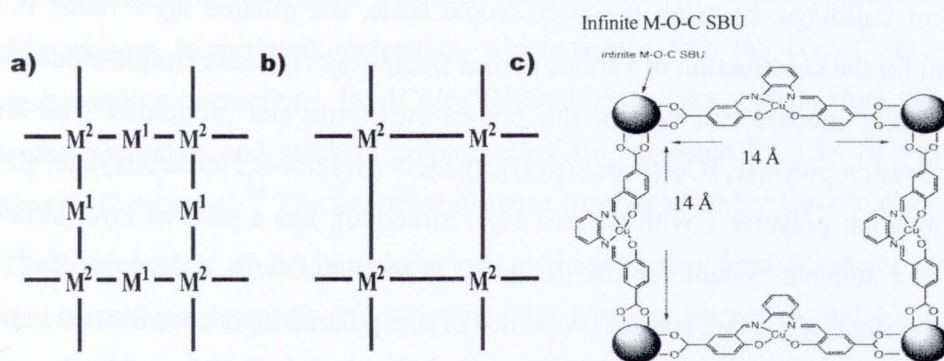


**Figure 1.6** Metal frameworks with a) two kinds of metal units (coordinatively saturated  $M^2$  and unsaturated  $M^1$ ), and b) coordinatively saturated  $M^2$ , c) part of the structure of  $\{[Zn_3Cu_2(OH)_2(\text{salphdc})_2] \cdot 2\text{dmf}\}$ .

### 1.3 Porous Structures<sup>1</sup>

#### 1.3.1 Dots (0D Cavities)

Nanosized pores, which are isolated from the others and scattered in the solid, occur in several coordination-polymer solids and are divided into two categories: solid without windows and solids with windows, but these windows are very small compared to the guest molecules. In any case, guest molecules are unable to leave these cavities. An interpenetrated 3D network of  $\{[\text{Zn}(\text{CN})(\text{NO}_3)(\text{tpt})_{2/3}] \cdot 3/4\text{C}_2\text{H}_2\text{Cl}_4 \cdot 3/4\text{CH}_3\text{OH}\}_n$  ( $\text{tpt} = 2,4,6\text{-tri}(4\text{-pyridyl})\text{-}1,3,5\text{-triazine}$ ) provides a barrier impenetrable to even the smallest molecules (with the possible exception of  $\text{H}_2$ ), effectively isolating each cavity from its neighbors and from the outside world.<sup>22</sup> The cavities, sealed-off in this manner, are exceptionally spacious, the distance across the inner shell from one  $\text{Zn}_4$  square to the opposite and parallel  $\text{Zn}_4$  square is the unit cell length, 23.448(4) Å. The cavity is large enough to accommodate approximately nine 1,1,2,2-tetrachloroethane molecules, together with nine molecules of methanol, all of which are highly disordered and behave essentially like a liquid.

#### 1.3.2 Channels (1D Space)

A large number of coordination polymers with regular 1D channels have been synthesized and crystallographically characterized. Several sizes and shapes of 1D channel are known.

On the macroscopic scale, pillared layer structures are frequently been found in ancient buildings. Even on the microscopic scale, the pillared layer motif is very useful for the construction of various porous frameworks because simple modification of a pillar module can control the porous structures and properties. The Cu(II) coordination polymer,  $[\text{Cu}_2(\text{pzdc})_2(\text{pyz})]_n$  ( $\text{pzdc} = \text{pyrazine-}2,3\text{-dicarboxylate}$ , CPL-1; coordination polymer 1 with pillared layer structure), has a pillared layer structure, and is a suitable system for the design of porous structures and properties.<sup>23</sup> The channel dimensions and surface properties of this pillared layer coordination network can be controlled by modification of the pillar ligands. For this purpose, various pillar ligands, which have a variety of lengths and functionalities (Figure 1.7), were employed to yield a series of compounds,  $\{[\text{Cu}_2(\text{pzdc})_2\text{L}] \cdot n\text{H}_2\text{O}\}_n$  ( $\text{L} = \text{pyz}$  (CPL-1,  $n = 1$ ), **4,4'-bpy** (CPL-2,  $n = 4$ ),<sup>23</sup> *pyre* (CPL-3,  $n = 4$ ), *azpy* (CPL-4,  $n = 5$ ), *dpe*

(CPL-5,  $n = 4$ ),<sup>23</sup> and pia (CPL-6,  $n = 5$ )<sup>22</sup>). For such a series of compounds which have a similar basic framework, Rietveld analyses of the X-ray powder diffraction patterns are useful for structure determination. Modification of the pillar ligands enables us to realize systematic control not only of the pore size (approximately 8 x 6, 8 x 3, 10 x 6, and 10 x 6 Å<sup>2</sup> for **CPL-2**, **3**, **4** and **5**, respectively), but also of the surface functionality.

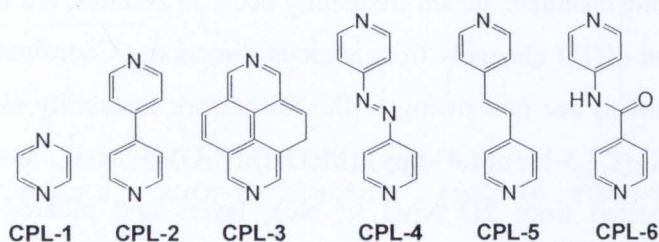


**Figure 1.7** Linker ligands used as pillars in  $\{[\text{Cu}_2(\text{pzdc})_2\text{L}] \cdot n\text{H}_2\text{O}\}_n$ . (pzdc = pyrazine-2,3-dicarboxylate)

### 1.3.3 Layers (2D Space)

While there are dozens of 2D coordination polymers, only a few have been reported in which several guests can be incorporated between the layers. The 1D motif of  $\{\text{Cu}(\text{ca})(\text{ROH})_2\}$  (ca = chloranilate) contains hydrogen-bonding sites, ca-O (hydrogen-bond acceptor) and ROH (hydrogen-bond donor).<sup>24</sup>  $[\text{Cu}(\text{ca})(\text{H}_2\text{O})_2]$  has a layer structure and the distance between the copper atoms in the different sheets is 8.45 Å. In fact, the compound obtained,  $[\text{Cu}(\text{ca})(\text{H}_2\text{O})_2]$ , is thermodynamically unstable without intercalated molecules, which tightly link the layers<sup>25</sup> through hydrogen-bonding interactions. In  $\{[\text{Cu}(\text{ca})(\text{H}_2\text{O})_2] \cdot \text{phz}\}_n$  (phz = phenazine) the phz molecules intercalate and stack in columns that are separated by 3.18 Å (nearest neighbor C...C distance).<sup>25</sup> The interlayer distance (nearest neighbor Cu...Cu distance) is 9.25 Å. Molecules of 2,5-dimethylpyrazine (dmpyz) also form columnar stacks between the sheets. Interestingly, there are two types of phases (a and b) in the compound,  $\{[\text{Cu}(\text{ca})(\text{H}_2\text{O})_2] \cdot \text{dmpyz}\}_n$ . In the a- and b-phases, the stacking mode of dmpyz is similar, whereas the coordination mode of dmpyz is different and the two phases have different colors. This result also indicates that the layer spacing is flexible, a characteristic of coordination polymer frameworks. The spacing between

the layers in  $\{[\text{Cu}(\text{ca})(\text{H}_2\text{O})_2]_n\}_m$ , ranges from 8.45 to 11.0 Å. The intercalation is governed by 2 main factors: The intercalated molecule has 1) a  $\pi$ -electron structure allowing to form a stacked column, and 2) hydrogen-bonding sites in opposing directions for linking the layers.

### 1.3.4 Intersecting Channels (3D Space)

3D intersecting channels, which frequently occur in zeolites, are constructed by the interconnection of 1D channels from various directions. Coordination polymers with such 3D channels are rare owing to the framework instability associated with high porosity.  $\{[\text{Ni}_6(1,3,5\text{-btc})_4(\mathbf{4,4'}\text{-bpy})_6(\text{MeOH})_3(\text{H}_2\text{O})_9]\cdot\text{guest}\}_n$  has a 3D porous framework constructed from 2D  $\text{Ni}_3(1,3,5\text{-btc})_2$  layers and pillared by **4,4'-bpy** ligands, which gives hexagonal-shaped channels (12.3 and 11.0 Å in diameter) running parallel to the stacking direction. In addition, there are three 1D channels ( $8 \times 4.4 \text{ \AA}^2$ ) between the layers, forming an overall 3D framework of intersecting channels. In  $\{[\text{Zn}_4\text{O}(1,4\text{-bdc})_3]\cdot 8\text{dmf}\cdot\text{C}_6\text{H}_5\text{Cl}\}_n$  (IRMOF-1; IRMOF = isoreticular metal-organic framework), octahedral Zn-O-C units are linked by benzene supports to afford a primitive cubic structure (the B net in  $\text{CaB}_6$ ) and an exceptionally rigid and highly porous structure with 3D intersecting channels. The simple and facile synthetic method indicates that the use of other dicarboxylate linkers under similar conditions would yield the same type of frameworks with diverse pore sizes and functionalities. Indeed, using linkers other than 1,4-bdc yielded IRMOF-2 through to IRMOF-16 (Figure 1.8). In IRMOF-2 through IRMOF-7, 1,4-bdc linkers with bromo, amino, *n*-propoxy, *n*-pentoxy, cyclobutyl, and fused benzene functional groups were introduced into the desired structure in which their substituent groups point into the voids. Some of the IRMOFs have mesopores ( $>20 \text{ \AA}$ ) and have the lowest crystal density of any material reported to date.

## 1.4 Functions of Coordination Polymers<sup>1</sup>

### 1.4.1 Overview of Microporous Properties

Porous properties have attracted the attention of chemists, physicists, and material scientists because of not only industrial applications, such as separation, heterogeneous catalysis, and gas storage, but also because of scientific interest in the

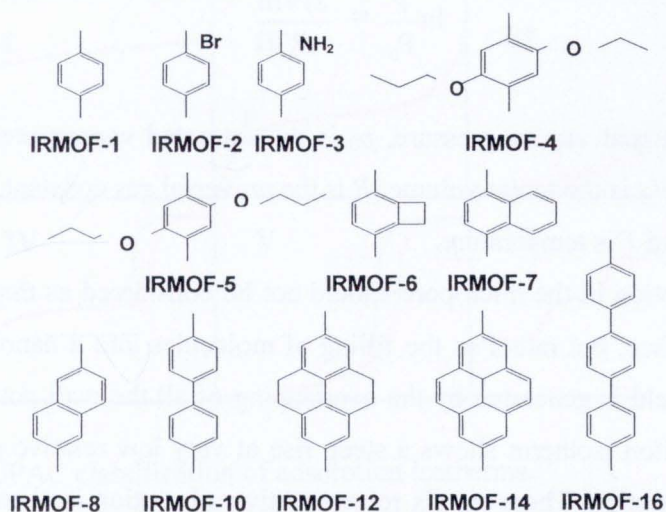


**Figure 1.8** Dicarboxylate linkers used in the preparation of IRMOF materials.

formation of molecular assemblies, such as clusters and 1D arrays, and in the anomalous physical properties of confined molecules can be studied. The adsorption of guest molecules onto the solid surface plays an essential role in determining the properties of porous compounds. This adsorption is governed not only by the interaction between guest molecules and the surfaces, but also by the pore size and shape. Pores are classified according to their size as shown in Table 1.1.<sup>26</sup> There is no essential difference between adsorption by a macropore and adsorption onto a single surface, and both are explained well by the Brunauer–Emmett–Teller (BET) equation.<sup>27</sup>

$$\frac{1}{v[(P_0/P) - 1]} = \frac{c-1}{v_m c} \left( \frac{P}{P_0} \right) + \frac{1}{v_m c}$$

$P$  and  $P_0$  are the equilibrium and the saturation pressure of adsorbates at the temperature of adsorption,  $v$  is the adsorbed gas quantity (for example, in volume units), and  $v_m$  is the monolayer adsorbed gas quantity.  $c$  is the BET constant.

The adsorption by a mesopore is dominated by capillary condensation, which is responsible for a sharp adsorption rise around the mid relative-pressure region. This effect is not attributable to molecule–solid interactions, but to a purely geometrical requirement, which is illustrated well by the Kelvin equation.<sup>28</sup>

$$\ln \frac{P}{P_0} = \frac{2\gamma V_m}{rRT}$$

where  $p$  is the actual vapour pressure,  $p_0$  is the saturated vapour pressure,  $\gamma$  is the surface tension,  $V_m$  is the molar volume,  $R$  is the universal gas constant,  $r$  is the radius of the droplet, and  $T$  is temperature.

The adsorption in the micropore should not be considered as that of molecules onto a solid surface, but rather as the filling of molecules into a nanospace where a deep potential field is generated by the overlapping of all the wall potentials. In this case, the adsorption isotherm shows a steep rise at very low relative pressure and a plateau after saturation. There are six representative adsorption isotherms that reflect the relationship between porous structure and sorption type.<sup>29</sup> The IUPAC classification of these adsorption isotherms is shown in Figure 1.9. These adsorption isotherms are characteristics of adsorbents that are microporous (type **I**), nonporous and macroporous (types **II**, **III**, and **VI**), and mesoporous (types **IV** and **V**). The differences between types **II** and **III** and between types **IV** and **V** arise from the relative strength of fluid–solid and fluid–fluid attractive interactions. When the fluid–solid attractive interaction is stronger than that of fluid–fluid, the adsorption isotherm should be of types **II** and **IV**, and opposite situation leads to types **III** and **V**. The type **VI** isotherm represents adsorption on nonporous or macroporous solid surfaces where stepwise multiplayer adsorption occurs. Many articles have been published on the adsorption processes in zeolites and activated carbons.<sup>30</sup>

**Table 1.1** Classification of pores

Pore type	Pore size (Å)
Ultramicropore	< 5
Micropore	5 – 20
Mesopore	20 - 500
Macropore	> 500

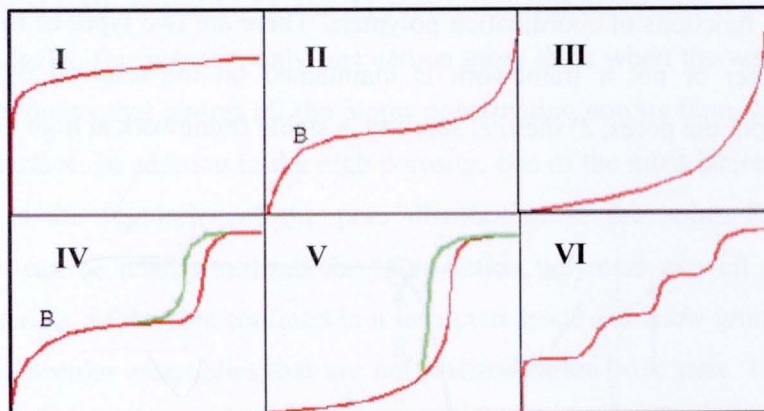


**Figure 1.9** IUPAC classification of adsorption isotherms.<sup>31</sup>

The six types of adsorption isotherms assume that the porous host structures are not altered through the sorption process. If the porous hosts have a flexible and dynamic nature, for example, when a structure transformation from nonporous to microporous occurs during the adsorption, the adsorption isotherm has a novel profile, dissimilar to the conventional type (Figure 1.9). In this case, the adsorption isotherm could be a combination of types **I** and **II** or **III**. In Figure 1.10, the adsorption isotherm follows the type **II** isotherm at low concentration (pressure), that of a nonporous phase. After a certain point A, the isotherm begins to approach type **I** with a sudden rise. At point B the structural transformation from nonporous to porous is complete. If many structural transformations occur, a multistep adsorption profile would be observed. This phenomenon is one of the advantages of coordination polymers with flexible and dynamic frameworks based on weak interactions, such as coordination bonds, hydrogen bonds,  $\pi$ - $\pi$  stacking interactions, and van der Waals forces. Structural flexibility accompanied with a certain structural transformation can even occur in inorganic porous materials. Several examples of flexible inorganic networks are known. The structural change in inorganic networks, however, is not so drastic as that of coordination polymers because of their robust frameworks characteristic of strong bonds, such as Si/Al-O bonds. A framework in which the pore size could be changed by temperature was found in a zeolite containing octahedral and tetrahedral motifs. However, on guest adsorption the framework is not flexible, but robust. The structural stability is an important factor in the study of the

microporous functions of coordination polymers. There are two types of the stability: i.e. 1) whether or not a framework is maintained on the removal of the guest molecules from the pores, 2) thermal stability, a stable framework at high temperature tends to

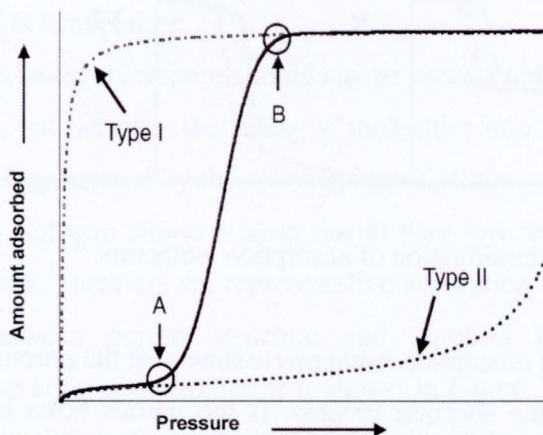


**Figure 1.10** Adsorption isotherms observed when porous frameworks undergo a structure transformation from nonporous to porous. Dashed lines represent the Type I and Type II isotherms. Points A and B indicate the gate-opening and gate-closing pressures which accompany the start and end of the structure transformation, respectively.

require strong bonding between building blocks, but in certain cases the stability depends on the mode of framework. X-ray powder diffraction (XRPD) and thermogravimetric (TG) measurements are commonly used to investigate the structural stability.

The specific surface area is one of the most important factors for evaluating the pore capacity, and is associated with the number of guest molecules accommodated by direct contact. Recently, the specific surface areas attainable with coordination polymers<sup>1,32,34</sup> have increased from  $500 \text{ m}^2\text{g}^{-1}$ , comparable to that of zeolites, to a very large value, i.e.  $4500 \text{ m}^2\text{g}^{-1}$ . This value is much higher than the ideal value of carbon materials,  $2630 \text{ m}^2\text{g}^{-1}$ , which is calculated as the sum of two surfaces of graphite planes. In practice, the thinner the walls of the pores are, the higher the specific surface area is. In the case of inorganic zeolites, the pore walls are constructed with a

thickness of at least several Si, O, and Al atoms, whereas coordination polymers may afford thin walls, for instance, only one carbon atom thick when the wall is of **4,4'-bpy**, which shows that almost all the atoms constructing porous frameworks can be used as a surface. In addition to the high porosity, one of the most interesting porous properties is the regularity of the pore distribution in the solid. Regular pore distribution can be readily realized for coordination polymers as well as inorganic porous materials. Molecules confined in a restricted space can show group properties and form molecular assemblies that are not realized in the bulk state. Utilization of this nanosized space found in precisely designed uniform pores has just begun.

## 1.4.2 Robust Frameworks Generating Nanospace<sup>1,2</sup>

### 1.4.2.1 Gas Storage

The ability to store a desired compound is a typical property of porous materials. The adsorption of gases at ambient temperature is important for applications, such as storage and transport. A useful strategy for the creation of suitable adsorbents is to prepare stable frameworks without guest molecules (2<sup>nd</sup> generation compounds). The first report on the gas-adsorption properties of those compounds at ambient temperature appeared in 1997. The framework reported is best described as a tongue-and-groove (bilayer) structure,  $\{[M_2(\mathbf{4,4'-bpy})_3(\text{NO}_3)_4] \cdot x\text{H}_2\text{O}\}_n$  ( $M = \text{Co}$ ,  $x=4$ ;  $\text{Ni}$ ,  $x=4$ ;  $\text{Zn}$ ,  $x=2$ ), formed from  $M(\text{NO}_3)_2$  and **4,4'-bpy** units (Figure 1.11a).<sup>32</sup> The effective micropore cross section for the dried sample is about  $3 \times 6 \text{ \AA}^2$  (based on van der Waals radii; Figure 1.11a). This host reversibly adsorbs  $\text{CH}_4$ ,  $\text{N}_2$ , and  $\text{O}_2$  in the pressure range of 0–36 atm without collapse of the crystal framework (Figure 1.11b). Similar coordination polymers capable of the gas adsorption have since been synthesized.<sup>33</sup> The adsorption of  $\text{N}_2$  or Ar gas at low temperature is generally used for the evaluation of micropores. The  $\text{N}_2$  adsorption isotherms measured at 77 K on CPL-1, CPL-2, and CPL-5 are given in Figure 1.12.<sup>34</sup> All CPL samples show typical isotherms of type **I**, which confirms the presence of micropores and the absence of mesopores. The almost vertical rise of the  $\text{N}_2$  adsorption isotherms at low relative pressures indicates that the size of micropores is extremely uniform, which is characteristic of coordination polymers.

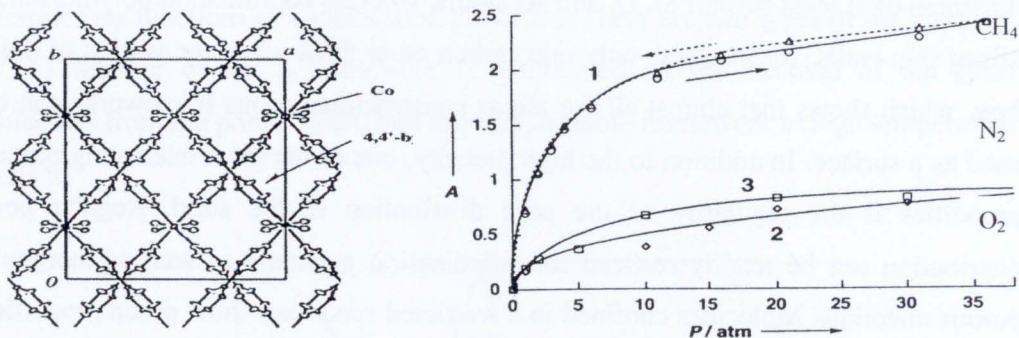


**Figure 1.11** a) view of  $\{[\text{Co}_2(4,4'\text{-bpy})_3(\text{NO}_3)_4] \cdot 4\text{H}_2\text{O}\}_n$ , along the  $c$  axis, b) isotherms of the adsorption of  $\text{CH}_4$ ; open triangle,  $\text{N}_2$ , and  $\text{O}_2$  by  $[\text{Co}_2(\text{NO}_3)_4(4,4'\text{-bpy})_3]_n$  at 298 K in the range 1–36 atm.

Methane is the main component of natural gas, which is an important candidate for clean transportation fuels. The storage of methane by adsorbents has been pursued vigorously as an alternative to compressed gas storage at high pressure. However, none of the conventional adsorbents have afforded sufficient  $\text{CH}_4$  storage to meet the conditions required for commercial viability. Even in activated carbons with large specific surface area and micropores, a high percentage of the mesopores and macropores are not effective for  $\text{CH}_4$  adsorption, because the single surface cannot trap  $\text{CH}_4$  molecules and therefore the large voids are useless. To achieve higher adsorption capacity, it is necessary to ensure that micropores with sizes well suited to methane molecules are densely and uniformly distributed in the solid. Porous coordination polymers are therefore good candidates as adsorbents for  $\text{CH}_4$  storage.

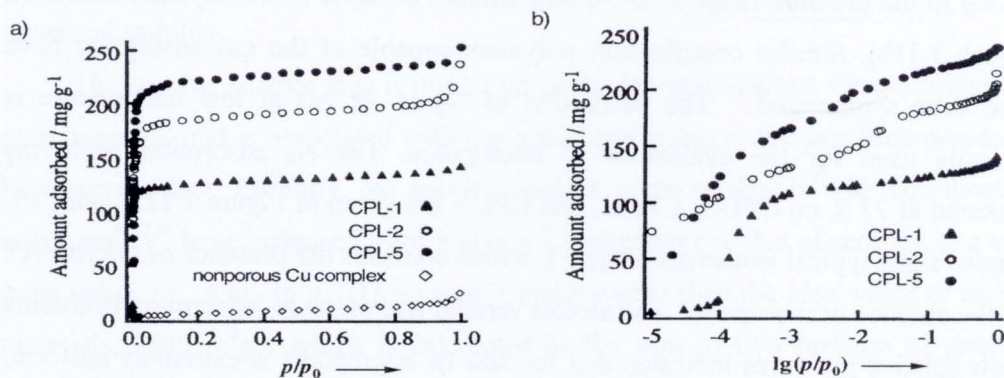


**Figure 1.12** a) Adsorption isotherms and b) the logarithmic relative pressure expression of adsorption isotherms of  $\text{N}_2$  on CPL-1, CPL-2 and CPL-5.

CH<sub>4</sub> gas adsorption for porous coordination polymers was first reported for  $\{[\text{Co}_2(\mathbf{4,4'}\text{-bpy})_3(\text{NO}_3)_4]\cdot 4\text{H}_2\text{O}\}_n$ , which adsorbs an equivalent of about 52 cm<sup>3</sup> (STP)g<sup>-1</sup> (STP = standard temperature and pressure) of CH<sub>4</sub> at a temperature of 298 K and a pressure of 30 atm (Figure 1.11b).<sup>32</sup> In 3D pillared-layer coordination polymers, CPL-1, CPL-2, and CPL-6, approximately 18, 56, and 65 cm<sup>3</sup> (STP)g<sup>-1</sup> of CH<sub>4</sub> are adsorbed at 298 K and 31 atm. The triply interpenetrated framework of  $\{[\text{Cd}_2(\text{NO}_3)_4(\text{azpy})_3]\cdot 2\text{Me}_2\text{CO}\}_n$ , which has microporous channels despite the interpenetration, also adsorbs a certain amount of CH<sub>4</sub> (40 cm<sup>3</sup> (STP)g<sup>-1</sup> at 298 K and 36 atm.

Recently, other types of compounds with high methane capacity have been synthesized. IRMOF-6, affords a 3D cubic porous network and has a high surface area, 2630 m<sup>2</sup>g<sup>-1</sup>, estimated by applying the Langmuir equation.<sup>35</sup> The CH<sub>4</sub> adsorption isotherm was found to have an uptake of 240 cm<sup>3</sup> (STP)g<sup>-1</sup> (156 cm<sup>3</sup> (STP)cm<sup>3</sup>) at 298 K and 36 atm (Figure 1.13). Based on volume, the amount of methane adsorbed by IRMOF-6 at 36 atm is about 70% of the amount stored in gas cylinders where much higher pressures (205 atm) are used. The size about 12 x 12 Å<sup>2</sup> provides the optimal fit for CH<sub>4</sub> molecules and the potential is thus sufficiently deep for the storage of methane.

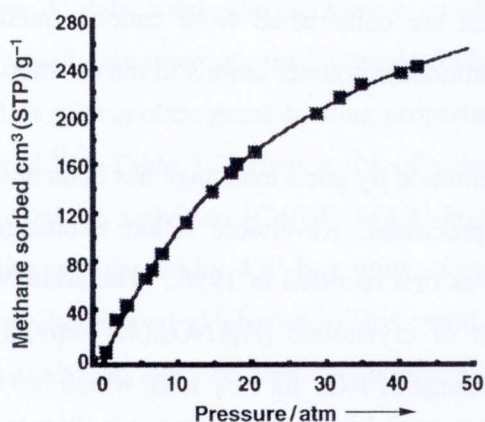


**Figure 1.13** Adsorption isotherm of CH<sub>4</sub> gas in IRMOF-6 fitted with the Langmuir equation at 298 K.

Hydrogen (H<sub>2</sub>) has attracted a great deal of attention as an energy source. Once it is generated, its use as a fuel creates neither air pollution nor greenhouse-gas emissions. However, no practical means for H<sub>2</sub> storage and transportation have yet been developed. So, the development of H<sub>2</sub>-fueled vehicles and portable electronics will require new materials that can store large amounts of H<sub>2</sub> at ambient temperature and relatively low pressures, with small volume, low weight, and fast kinetics for recharging. Metal hydride systems,<sup>36</sup> zeolites,<sup>37</sup> and various carbon-based adsorbents<sup>38</sup> have been intensely examined in this respect. Very recently, H<sub>2</sub> adsorption has been carried out with the microporous Zn(II)-cluster-dicarboxylate coordination polymers, MOF-5, IRMOF-6, and IRMOF-8 as well as nickel(II) phosphates. The data from temperature programmed desorption (TPD) and inelastic neutron scattering (INS) measurements strongly suggest that nickel(II) phosphate has coordinatively unsaturated Ni(II) sites accessible to H<sub>2</sub> molecules in the pores.<sup>38</sup> MOF-5 adsorbs up to 4.5 weight% of H<sub>2</sub> (17.2 H<sub>2</sub> molecules per formula unit) at 78 K and 1.0 weight% at room temperature and a pressure of 20 atm.<sup>9</sup>

#### 1.4.2.2 Exchange

Porous zeolites have cation-exchange properties as a result of their anionic frameworks. Porous coordination polymers in contrast to zeolites tend to have cationic frameworks, which are constructed from cationic metal ions and neutral bridging ligands, and accommodate counter anions in the cavities, and therefore have anion-exchange properties.<sup>4</sup>

Crystal transformation by guest exchange has been mainly observed in the case of anion-exchange processes. Reversible anion exchange accompanying a structural transformation was first reported in 1996.<sup>39</sup> The addition of a slight excess of NaPF<sub>6</sub> to a suspension of crystalline [Ag(NO<sub>3</sub>)(4,4'-bpy)]<sub>n</sub> in water at room temperature causes the exchange of NO<sub>3</sub><sup>-</sup> for PF<sub>6</sub><sup>-</sup> ions, which is 95% complete after 6 h. [Ag(edtpn)(NO<sub>3</sub>)]<sub>n</sub>, which affords a 1D coordination polymer, undergoes anion-dependent rearrangement with re-coordination of the Ag(I) center.<sup>40</sup> During the anion exchange the supramolecular structural transformations between [Ag(edtpn)(NO<sub>3</sub>)]<sub>n</sub>, 2D-layer {[Ag(edtpn)]·CF<sub>3</sub>SO<sub>3</sub>}<sub>n</sub>, and the boxlike 2D-network {[Ag(edtpn)]·ClO<sub>4</sub>}<sub>n</sub>, are observed in the crystalline state (Figure 1.14).

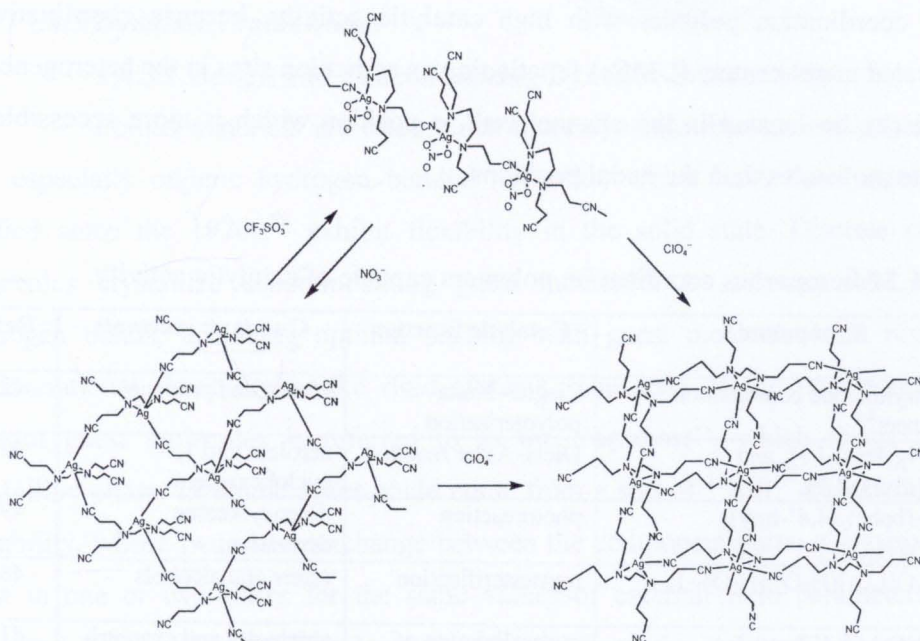


**Figure 1.14** Structural rearrangement through anion exchange in  $[Ag(edtpn)(NO_3)]_n$ .

### 1.4.2.3 Catalysts

Metal ions play key roles in organic transformations, which are usually carried out with soluble species in a homogeneous solution. An advantage of heterogeneous catalysts is their ready recoverability; they are important in industry applications. However, to date, solid catalysts have been almost exclusively inorganic materials. Especially useful are microporous inorganic zeolites. Despite recent interest in metal–organic solids with zeolitic guest-binding properties, their catalytic activities are largely unexplored.<sup>41–55</sup> Table 1.2 gives a list of porous coordination polymers with heterogeneous catalytic activities.  $[Cd(NO_3)_2(4,4'\text{-bpy})_2]_n$ , which consists of 2D networks with cavities surrounded by **4,4'-bpy** units, shows shape-specific catalytic activity for the cyanosilylation of aldehydes.<sup>41</sup> This reaction is apparently promoted by the heterogeneous polymer, since no reaction takes place with powdered  $Cd(NO_3)_2$  or **4,4'-bpy** alone, or with the supernatant liquid from a  $CH_2Cl_2$  suspension of the coordination polymer. A homochiral open-framework solid,  $\{[Zn_3O(L)_6](H_3O)_2(H_2O)_{12}]_n$  ( $L$  = chiral organic ligand), has enantioselective catalytic activity for transesterification.<sup>46</sup> The observed size selectivity suggests that the catalysis mainly occurs in the channels. Using a metalloligand as a building unit could provide a novel

porous coordination polymer with high catalytic activity, because coordinatively unsaturated metal centers (UMCs) functioning as activation sites in the heterogeneous catalyst can be located in the channel wall, a position which is more accessible to substrate molecules than the nodal positions.

**Table 1.2** Microporous coordination polymers capable of catalytic activity

Compound <sup>a</sup>	Catalytic function	Guests or reactants	Ref.
Ti <sup>IV</sup> aryldioxide coordination polymers <sup>b,c</sup>	Ziegler–Natta polymerization	ethene and propene	42
[Ti <sub>2</sub> Cl <sub>2</sub> ( <i>i</i> PrO) <sub>2</sub> L1] <sub>n</sub> and [Zr <sub>2</sub> ( <i>t</i> BuO) <sub>4</sub> L1] <sub>n</sub> <sup>d</sup>	Diels–Alder reaction	acrolein and 1,3-cyclohexadiene	47
{[Co <sub>3</sub> (bpbcb) <sub>3</sub> (4,4'-bpy)](dmf) <sub>4</sub> (H <sub>2</sub> O)} <sub>n</sub>	photoreaction	dibenzylketone derivatives	49
{[Zn <sub>3</sub> O(L <sub>2</sub> ) <sub>6</sub> ](H <sub>3</sub> O) <sub>2</sub> (H <sub>2</sub> O) <sub>12</sub> } <sub>n</sub>	transesterification	esters and alcohols	46
[Cd(NO <sub>3</sub> ) <sub>2</sub> (4,4'-bpy) <sub>2</sub> ] <sub>n</sub>	cyanosilylation of aldehydes	aldehydes and cyanotri-methylsilane	41
[In <sub>2</sub> (OH) <sub>3</sub> (1,4-bdc) <sub>1.5</sub> ] <sub>n</sub> <sup>e</sup>	hydrogenation of nitroaromatics and oxidation of sulfides	nitrobenzene, 2-methyl-1-nitronaphthalene, methyl phenylsulfide, and (2-ethylbutyl) phenylsulfide	43
{[Ru(1,4-diisocyanobenzene) <sub>2</sub> ](Cl) <sub>2</sub> } <sub>n</sub> <sup>d</sup>	hydrogenation and isomerization	1-hexene	50,51
[RhL] <sub>n</sub> (L = fumarate and 1,4-bdc)	hydrogen exchange	ethene, propene, butene, and hydrogenation	44
PdII coordination polymer gels <sup>d</sup>	oxidation of benzylalcohol	benzylalcohol	45
{[Ln(H <sub>2</sub> L <sub>3</sub> )(H <sub>3</sub> L <sub>3</sub> )(H <sub>2</sub> O) <sub>4</sub> ]•xH <sub>2</sub> O} <sub>n</sub> (Ln = La, Ce, Pr, Nd, Sm, Tb; x = 9–14)	cyanosilylation of aldehydes and ring opening of <i>meso</i> -carboxylic anhydrides	aldehydes and cyanotri-methylsilane, <i>meso</i> -2,3-dimethylsuccinic anhydride	48
[Cd <sub>3</sub> L <sub>4</sub> (NO <sub>3</sub> ) <sub>6</sub> ]•7MeOH•5H <sub>2</sub> O	Addition of diethylzinc	aldehydes and diethylzinc	52
[Sc <sub>2</sub> (C <sub>8</sub> H <sub>4</sub> O <sub>4</sub> ) <sub>3</sub> ]	oxidation of sulfides.	methyl phenyl sulfide	53
Cu <sub>3</sub> (BTC) <sub>2</sub> (H <sub>2</sub> O) <sub>3</sub> • xH <sub>2</sub> O	cyanosilylation of aldehydes	aldehydes and cyanotri-methylsilane	54
Mn <sub>3</sub> [(Mn <sub>4</sub> Cl) <sub>3</sub> (BTT) <sub>8</sub> (CH <sub>3</sub> OH) <sub>10</sub> ] <sub>2</sub>	cyanosilylation of aldehydes	aldehydes and cyanotri-methylsilane	55

<sup>a</sup> L1 = anthracenebisresorcinol derivative. L2 is chiral organic ligands. H<sub>4</sub>L<sub>3</sub> = 2,2'-diethoxy-1,1'-binaphthalene-6,6'-bisphosphonic acid; <sup>b</sup> Methylalumoxane (MAO) as cocatalyst; <sup>c</sup> aryldioxide=*p*-benzenedioxide, 2,7-naphthalenedioxide, and 4,4'-biphenyldioxide; <sup>d</sup> Exact crystal structures are not determined.; <sup>e</sup> Nonporous materials.



### 1.4.3 Dynamic Frameworks<sup>2</sup>

#### 1.4.3.1 Design and Functionalizing Dynamic Frameworks

Porous materials are often much more dynamic than generally believed, and especially organic hydrogen bonded networks, which have been extensively studied since the 1970s,<sup>56</sup> exhibit flexibility in the solid state. Discrete organic molecules crystallize accommodating guest molecules (= solvent) with elastic hydrogen bonds, achieving optimal packing with guest molecules and revealing conformational flexibility unlike rigid systems. The state of the host component without guest molecules is referred to as the “**apohost**”, which forms a new crystalline phase. Dynamic pores could come from a sort of “soft” framework with bistability, whose two states exchange between the component parts; a system could exist in one or two states for the same values of external field parameters. The structural rearrangement of molecules proceeds from the “closed” phase to the “open” phase responding to guest molecules as in eqn. (1).<sup>57</sup>



where H is apohost, G is guest molecule, and  $n$  is stoichiometry of accommodated guest vs. apohost (hereafter, the number  $n$  is defined as the ratio of [the amount of adsorbed guest molecules]/[asymmetric unit of the crystal]).

Compared with discrete ensembles (molecule- and/or ion-based compounds), the flexibility of coordination polymers has been overlooked for a long time. This is because, in general, flexibility appears incompatible with robustness, such that porous frameworks constructed from rigid components and linkage are maintained without guest molecules. Nevertheless, the importance of softness, *e.g.* elongation and shrinking with the accommodation of guest molecules, has been proposed and recognized in third generation coordination polymers (Figure 1.15 bottom).<sup>5,58</sup> Throughout the design, synthesis, and examination of robust porous coordination polymers, researchers have come to a better understanding that a certain coordination bond could not only sustain a porous framework, but also transform the framework into a different one. In particular, coordination polymers have acquired softness for their porous frameworks in cooperation with weak bonds, such as hydrogen bonds



and/or  $\pi$ - $\pi$  stacking interactions. So-called dynamic structural transformation based on flexible porous frameworks is one of the most interesting phenomena in coordination polymers, which are categorized as the three types in Figure 1.15.<sup>59</sup>

(1) A Type I framework of “recoverable collapsing” has the property that by removal of guest molecules a network collapses due to the close packing force, however it regenerates under the initial conditions.

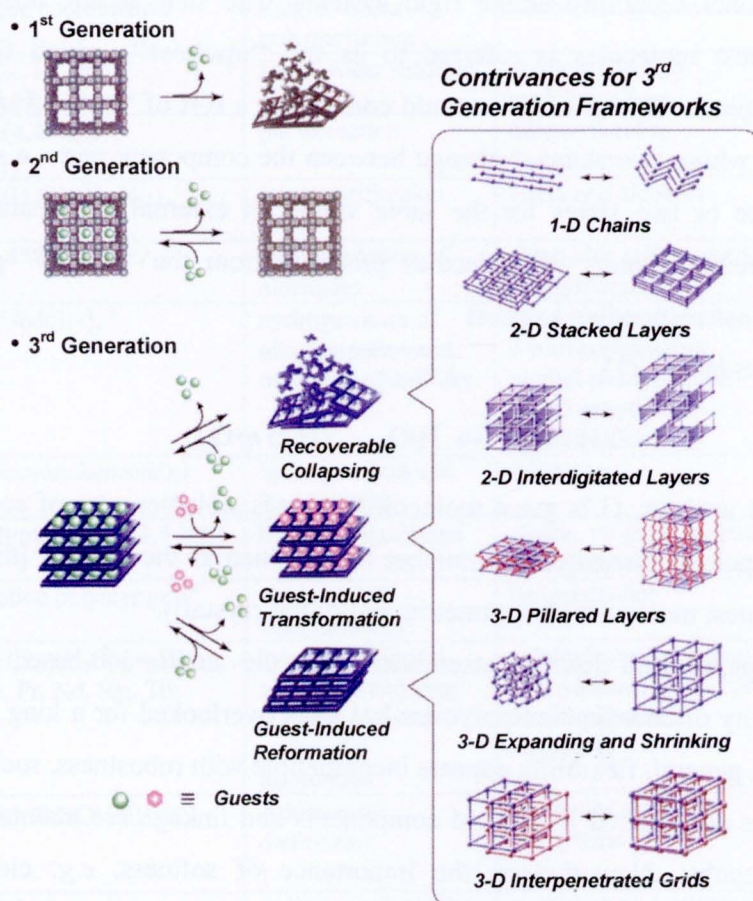


**Figure 1.15** Schematic view of first-, second-, third-generation microporous coordination polymers. Third-generation compounds are divided into three kinds of the classification, “recoverable collapsing”, “guest-induced transformation”, and “guest-induced reformation”, which are realized with flexible contrivances in coordination networks drawn after reference 2.

(2) A Type II framework of “guest-induced transformation” has the property that structural shifts in the network are induced by the simultaneous exchange of guest molecules.

(3) A Type III framework of “guest-induced reformation” has the property that removal of guest molecules makes a structural change in the network to a different one; however it reverts to the original one under the initial conditions.<sup>40,43</sup>

Type I is regarded as “crystal-to-amorphous transformation”, therefore, the approach used to create such a transformation could be applicable to brittle materials systems. Whereas Type II and III compounds show “crystal to crystal transformation”, “ $\mathbf{H} \supset n \bullet \mathbf{G} \leftrightarrow \mathbf{H} \supset n \bullet \mathbf{G}'$  (Type II; the crystallinity is different between  $\mathbf{H} \supset n \bullet \mathbf{G}$  and  $\mathbf{H} \supset n \bullet \mathbf{G}'$ )” and “ $\mathbf{H} \supset n \bullet \mathbf{G} \leftrightarrow \mathbf{H} \supset n \bullet \mathbf{G}$  (Type III; the crystallinity is different between  $\mathbf{H}$  and  $\mathbf{H} \supset n \bullet \mathbf{G}$ )”, in a sense, this property results from the advantage of the molecular inorganic–organic hybrid system. Type II is found in heterogeneous anion exchange, where the guests are anions. Needless to say, porous coordination polymers having similar crystalline phases between the apohost and adsorbed forms are recognized as 2<sup>nd</sup> generation compounds.

#### 1.4.3.2 Contrivance for Dynamic Porous Coordination Polymers

A guideline for rigid pores in coordination polymers is that stiff building units are linked with strong chemical bonds such as coordination and/or covalent bonds to form a 3D framework. Dynamic pores, however, are subject to another constraint to give a flexible sort of framework, that is, building units (or motifs) with flexible moieties are linked with strong bonds, or stiff building blocks (or motifs) are connected with weaker bonds. Another possible option is the combination of flexible building blocks (motifs) and weak linkages. The generation of a host framework that interacts with exchangeable guest species in a switchable fashion has implications for the generation of previously undeveloped advanced materials with applications in areas such as molecular sensing. For weak linkages, guest molecules readily give rise to changes in bond direction, distance, and to cleavage. It is worth noting that even weak interactions between guest and pore-wall molecules can induce a structural change, because of a cooperative effect based on a large ensemble over an infinite framework. Coordination polymers form infinite networks, therefore extensive

cooperativity would be expected between the molecules throughout the crystal, such that rearrangement can occur in a well-concerted fashion, in order to maintain its macroscopic integrity.

For the construction of dynamic porous coordination polymers, it is necessary to consider certain devices based on weaker interactions, such as van der Waals forces,  $\pi$ - $\pi$  stacks, and hydrogen bonds etc. among the macroscopic integrities. One feasible idea is that a weak interaction device is put in between motifs (1D, 2D, and 3D), forming a contrivance for dynamic coordination polymers, which are grouped as shown in Figure 1.15;

(1) **1D motifs (chains)** are packed in a crystal, of which voids are accommodated by small sized molecules. Those consisting of silver(I) and **4,4'-bpy** analogues have cationic frameworks and exhibit anion exchange with framework transformation.<sup>60</sup>

(2) **2D motifs (single-type layers)** are superimposed on each other with one of two types of stacking, edge-to-edge or staggered, where a weak interaction operates between the sheets. Modification of ligands, which constitute layers, could control the spatial dimensions of the grids, functionality of the channel interior, and the manner of stacking.<sup>59</sup> One typical example is a 2D layer  $[\text{Ni}(\text{NO}_3)_2(\text{L1})_2]_n$  (L1 = 4,4'-bis(4-pyridyl)biphenyl), which selectively includes o-xylene from xylene isomers, taking advantage of the sliding layers against neighboring layers.<sup>61</sup>

(3) **2D motifs (interdigitated layers)** are superimposed on each other with ridges and hollows interlocked, to form 1D channels. These channels are in "closed form" without guests, whereas certain guest molecules could pass through them as a result of the framework's elongation.<sup>58</sup>

(4) **3D motifs (pillared layers)** have channels, whose interior properties are modulated by the judicious choice of layers and pillars. The reversible phenomena of interlayer elongation and shortening could be realized by non-rigid pillars; the channels are so flexible that the initial channels may re-form with guests even after their collapse without guests.<sup>58</sup>

(5) **3D motifs (expanding and shrinking grids)** show sponge-like dynamic behaviors, reducing the interior spacing dramatically in response to guest removal, and elongating it with the inclusion of guest molecules.<sup>62</sup>



(2) *Breathing type pores*: The expansion makes a guest molecule fit tightly into the host when the size of the pore is smaller than the guest molecule.<sup>64</sup>

(3) *Guest-exchange deformation type pores*: The pore shape is induced to change responding to guest shape in a simultaneous guest exchange.<sup>65</sup>

(4) *Healing type pores*: The collapsed pore in the absence of guest molecules are regenerated while the guests accommodate.<sup>66</sup>

The pores observed in type (1)/(3) exhibit the “open to- open” deformation accompanying with guests inclusion. On the other hand, the pores in type (2)/(4) exhibit “close-to-open” deformation, and it is worth noting that type (1) and (2) and in opposite manner. Needless to say, type (3) and (4) are associated with “guest-induced transformation (type-II)” and “guest-induced reformation (type-I)”, respectively (see also Figure 1.15).

### 1.5 The Monocarboxylate Ligands

The monocarboxylate ligands are known to assume many types of bridging conformations.<sup>67</sup> The following important coordination modes of monocarboxylate are shown in Figure 1.17. In addition, monocarboxylate anions exhibit a versatile coordination behavior displaying distinct bonding modes toward metal cations, such as monodentate and chelate, as well as  $\eta^1:\eta^1:\mu$  bridging ligands in *syn,syn*, *syn,anti*, and *anti,anti* conformations. Another type of coordination mode is the monoatomic bridge in which two metal ions are connected by a single oxygen atom of a carboxylate group. This diversity of coordination modes assumed by monocarboxylate ligands is summarized in Figure 1.17.

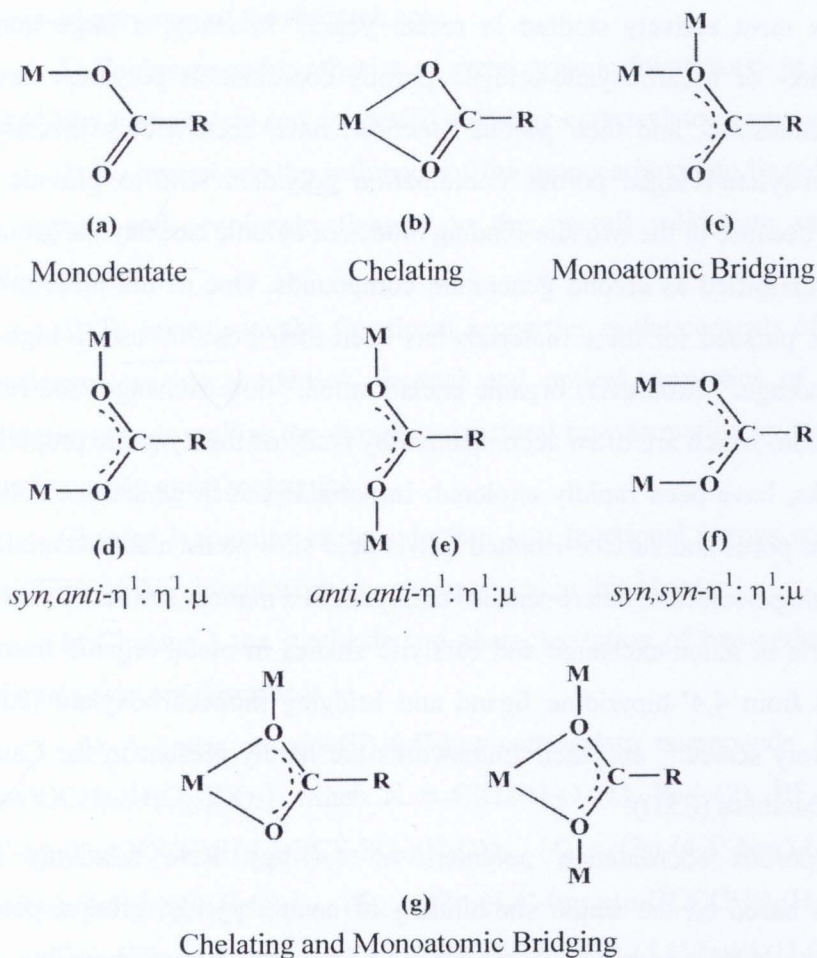


**Figure 1.17** Structurally characterized coordination modes of monocarboxylate ligand.

### 1.6 Aims of the Present Work

Porous coordination polymers (PCPs), also known as metal-organic frameworks (MOFs) have attracted intensive attention for the past decade owing to their diverse topologies and enormous potential applications for molecular storage and separation, catalysis, and ion exchange.<sup>1-9</sup> The porous coordination polymers have advantages in that they provide not only light materials with high porosity, but also desirable regular networks. Despite the extensive studies, application of porous compounds is still quite limited compared to that of zeolites. The coordination networks with cavities and

channels is most actively studied in recent years.<sup>9</sup> Recently, a large number of dicarboxylate- or tricarboxylate-bridged porous coordination polymers have been hitherto synthesized, and their porous functions have been widely investigated.<sup>2-8</sup> These carboxylate-bridged porous coordination polymers tend to provide a rigid framework because of the two site-binding modes of anionic carboxylate groups, they have been classified as second generation compounds. One of the more prominent applications pursued for these materials has been their possible use in high-density hydrogen storage.<sup>68</sup> Moreover, organic enclathration,<sup>68</sup> ion exchange, and reversible gas absorption, which are often accompanied by study of the dynamic properties<sup>69</sup> of the networks, have been rapidly explored. Importantly, such crystalline solids with well-defined pores and surface-isolated Lewis acid sites could also potentially serve as size- or shape-selective heterogeneous catalysts, in a manner similar to zeolites.

Reports of anion-exchange and catalytic studies in metal-organic frameworks constructed from 4,4'-bipyridine ligand and bridging monocarboxylate units have been relatively scarce.<sup>69</sup> and their frameworks are hardly present in the Cambridge Structural Database (CSD).

The porous coordination polymers of **4,4'-bpy** have relatively flexible frameworks based on the single site-binding of neutral pyridyl groups, potentially affording the third generation compounds. Moreover, monocarboxylate ligands exhibit several coordination modes to the metal center leading to a variety of polynuclear compounds ranging from discrete entities to multi-dimensional systems. From this background, the coordination polymers have been extended to develop a new type of coordination polymer assembled from the combination of **4,4'-bpy** and monocarboxylate-regulator as a bridge and transition metal ions, in which the framework motif is due to the topology of both ligands and the preferent geometry of metal centers.

The main purposes of the research are

1) To design and synthesize of metal organic frameworks in a series of zinc(II)-**4,4'-bpy**-carboxylato and copper(II)-**4,4'-bpy**-carboxylato compounds.

2) To investigate the influence of the monocarboxylato ligands, namely formato, acetato and propionato ligands on the overall solid-state structure of coordination polymers.

3) To investigate the functional properties in the contexts of catalysis, anion exchange, sensing properties, thermal and optical properties of the metal organic frameworks as well as the dynamic structural transformation by removal and reintroduction of the guest molecules.

Chapter 1 contains an introduction into functional porous coordination polymers. Aims of the present work are also reported in this chapter.

In Chapter 2 the synthesis and characterization of two series of metal organic frameworks are described:

1) A series of zinc(II)-**4,4'-bpy**-carboxylato compounds  $\{[\text{Zn}_3(\mathbf{4,4'-bpy})_{3.5}(\mu\text{-OOCH})_4(\text{H}_2\text{O})_2](\text{X})_2\}_n$  when  $\text{X} = \text{ClO}_4^- \cdot \text{H}_2\text{O}$  (1),  $\text{PF}_6^-$  (2),  $\text{BF}_4^- \cdot \text{H}_2\text{O}$  (3),  $\{[\text{Zn}(\mathbf{4,4'-bpy})(\mu\text{-OOCH})(\text{H}_2\text{O})_2](\text{CF}_3\text{SO}_3)(\text{H}_2\text{O})\}_n$  (4),  $\{[\text{Zn}_4(\mathbf{4,4'-bpy})_4(\mu\text{-OOCH})_5(\text{H}_2\text{O})_5](\text{NO}_3)_3(\mathbf{4,4'-bpy})_2(\text{H}_2\text{O})_3\}_n$  (5),  $\{[\text{Zn}_3(\mathbf{4,4'-bpy})_3(\mu\text{-OOCCH}_3)_4(\text{H}_2\text{O})_2](\text{PF}_6)_2(\text{H}_2\text{O})_2\}_n$  (6),  $\{[\text{Zn}_3(\mathbf{4,4'-bpy})_4(\mu\text{-OOCCH}_2\text{CH}_3)_4](\text{ClO}_4)_2(\mathbf{4,4'-bpy})_2(\text{H}_2\text{O})_4\}_n$  (7),  $\{[\text{Zn}_3(\mathbf{4,4'-bpy})_4(\mu\text{-OOCCH}_2\text{H}_5)_4(\text{H}_2\text{O})_2](\text{PF}_6)_2(\text{H}_2\text{O})_2\}_n$  (8),  $\{[\text{Zn}_2(\mathbf{4,4'-bpy})_2(\mu\text{-OOCCH}_2\text{H}_5)_2(\text{OH})(\text{H}_2\text{O})](\text{BF}_4)(\text{H}_2\text{O})_2\}_n$  (9),  $\{[\text{Zn}_2(\mathbf{4,4'-bpy})_2(\mu\text{-OOCCH}_2\text{H}_5)_2(\text{H}_2\text{O})_2](\text{CF}_3\text{SO}_3)_2\}_n$  (10)  $\{[\text{Zn}_3(\mathbf{4,4'-bpy})_4(\mu\text{-OOCCH}_2\text{H}_5)_4(\text{H}_2\text{O})_2](\text{NO}_3)_2(\text{H}_2\text{O})_3\}_n$  (11) and

2) A series of copper(II)-**4,4'-bpy**-carboxylato compounds  $\{[\text{Cu}_3(\mathbf{4,4'-bpy})_2(\mu\text{-OOCH})_4(\text{H}_2\text{O})_2](\text{X})_2(\text{H}_2\text{O})_6\}_n$  when  $\text{X} = \text{ClO}_4^-$  (12),  $\text{PF}_6^-$  (13),  $\text{BF}_4^-$  (14),  $\text{CF}_3\text{SO}_3^-$  (15),  $\{[\text{Cu}(\mathbf{4,4'-bpy})(\mu\text{-OOCH})(\text{NO}_3)]\}_n$  (16),  $\{[\text{Cu}_2(\mathbf{4,4'-bpy})_2(\mu\text{-OOCCH}_3)_3](\text{X})(\text{H}_2\text{O})\}_n$  when  $\text{X} = \text{ClO}_4^-$  (17),  $\text{PF}_6^-$  (18),  $\text{BF}_4^-$  (19),  $\text{CF}_3\text{SO}_3^-$  (20).

All products have been characterized by X-ray structure analysis, elemental microanalysis, infrared, electronic diffuse reflectance and EPR spectra as well as X-ray powder diffraction and reported as the preliminary results in chapter 2.

In Chapter 3 three porous coordination polymers, *i.e.* the three-dimensional framework,  $\{[\text{Zn}_3(\mathbf{4,4'}\text{-bpy})_{3.5}(\mu\text{-OOCH})_4(\text{H}_2\text{O})_2](\text{ClO}_4)_2(\text{H}_2\text{O})_2\}_n$  (**1**), the one-dimensional three-leg ladder  $\{[\text{Zn}_3(\mathbf{4,4'}\text{-bpy})_3(\mu\text{-OOCCH}_3)_4(\text{H}_2\text{O})_2](\text{PF}_6)_2(\text{H}_2\text{O})_2\}_n$  (**6**), and the two-dimensional layered network  $\{[\text{Zn}_3(\mathbf{4,4'}\text{-bpy})_4(\mu\text{-OOCCH}_2\text{CH}_3)_4](\text{ClO}_4)_2(\mathbf{4,4'}\text{-bpy})_2(\text{H}_2\text{O})_4\}_n$  (**7**) are structurally described in detail and compared with those of the remaining and other relevant coordination polymers. The thermal and optical properties, potential cation-exchange properties with structure retention by doping zinc(II) compounds with copper(II) and manganese(II), dynamic structural transformation by removal and reintroduction of guest molecules, anion-exchange and catalytic reactivity of all frameworks in a series of zinc(II)-**4,4'**-bpy-carboxylato compounds have been studied.

Chapter 4 describes the structures of two porous coordination polymers in a series of copper(II)-**4,4'**-bpy-carboxylato compounds, namely, the two-dimensional layered networks  $\{[\text{Cu}_3(\mathbf{4,4'}\text{-bpy})_3(\mu\text{-OOCH})_4(\text{H}_2\text{O})_2](\text{ClO}_4)_2(\text{H}_2\text{O})_6\}_n$  (**12**) and  $\{[\text{Cu}_2(\mathbf{4,4'}\text{-bpy})_2(\mu\text{-OOCCH}_3)_3](\text{PF}_6)(\text{H}_2\text{O})\}_n$  (**18**). They are structurally compared with those of the remaining and other relevant coordination polymers. The thermal and optical properties, dynamic structural transformation by removal and reintroduction of guest molecules, anion-exchange and catalytic reactivity of all porous coordination polymers in this series have been investigated. The crystals of  $\{[\text{Cu}_3(\mathbf{4,4'}\text{-bpy})_2(\mu\text{-OOCH})_4(\text{H}_2\text{O})_2](\text{X})_2(\text{H}_2\text{O})_6\}_n$  when  $\text{X} = \text{PF}_6^-$  (**13**),  $\text{CF}_3\text{SO}_3^-$  (**15**), and  $\{[\text{Cu}_2(\mathbf{4,4'}\text{-bpy})_2(\mu\text{-OOCCH}_3)_3](\text{X})(\text{H}_2\text{O})\}_n$  when  $\text{X} = \text{ClO}_4^-$  (**17**),  $\text{BF}_4^-$  (**19**),  $\text{CF}_3\text{SO}_3^-$  (**20**) appeared not good enough for X-ray structure analysis, thus the structures of these compounds have been proposed by elemental microanalyses and spectroscopic properties and are reported in this chapter.

Chapter 5 summarizes the research described in this thesis and presents an outlook to the future. Parts of this thesis have been published or submitted for publication.<sup>70,71</sup>